M2Di : MATLAB 2-D Stokes Solvers Using the Finite Difference Method

Ludovic.Raess@unil.ch[1] | Thibault Duretz[1] | Yuri Y. Podladchikov[1] | Stefan M. Schmalholz[1]

Scientific Computing Group | [1] Institute of Earth Sciences (ISTE) | University of Lausanne, Switzerland

Objectives and Methods

- M2Di: Mechanics 2-D iterative [Räss et al., 2017] in G-cubed.
- Linear and power law incompressible viscous flow based on the Finite-Difference Method.
- The codes are written in a concise vectorized MATLAB fashion and can achieve a time to solution of 22 s for linear viscous flow on 1000^2 grid points using a standard personal computer.
- Linear Stokes flow - Picard linearization: symmetric positive-definite matrix operators on Cartesian grids with either regular or variable grid spacing.
- Power law Stokes flow, both Picard and Newton (analytical Jacobian) iterations schemes are implemented.
- The M2Di routines are available from Bitbucket and the University of Lausanne Scientific Computing Group website:

SCAN ME

https://bitbucket.org/lraess/m2di
www.unil.ch/geocomputing/tools/software/m2di/

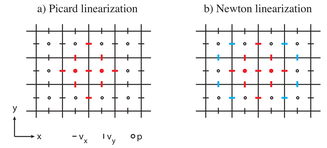

Fig. 1 | Examples of Finite Difference stencils used for discretizing the x-momentum equation. (a) the standard linear Stokes stencil (red symbols - Picard) and (b) the stencil arising from the Newton linearization (blue symbols) of the Stokes equation with power law rheology.

Benchmarks

> Validation of power law Stokes flow

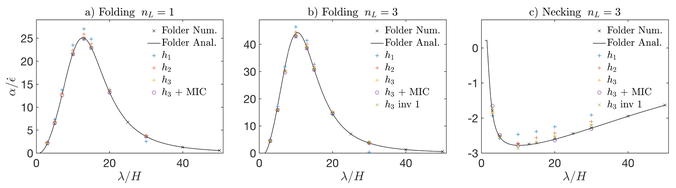

Fig. 2 | Numerically calculated growth rates $\alpha / \dot{\epsilon}_{II}$ for various types of mechanical instabilities: (a) linear viscous folding, (b) power law viscous folding, and (c) power law viscous necking. The results are compared to those obtained with the Folder toolbox [Adamuszek et al., 2016] (black dot and line). λ corresponds to the wavelength of the sinusoidal perturbation. The layer thickness H=1, the amplitude of the perturbation is set to 0.05, and the reference viscosity contrast is 200. Growth rates were calculated using three different grid resolutions. The highest resolution benchmark run, h_3, was also performed using a marker-in-cell (MIC) viscosity interpolation at the material interface and using the "inv 1" invariant formulation.

> Validation of linear Stokes flow

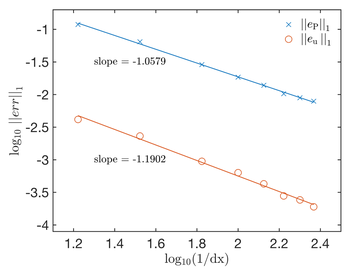

Fig. 3 | Evolution of velocity and pressure truncation errors (L1-norm) upon mesh refinement. The Finite Difference scheme is first-order accurate in space for both velocity and pressure. We have set the matrix viscosity to 1, and the inclusion viscosity to 10^4. Boundary conditions for the analytical solution were set to far-field pure shear. For the numerical solution, we use full Dirichlet boundary conditions where normal and tangential velocity components were analytically evaluated.

Linear and Power law Results

> Crystal-melt dynamics

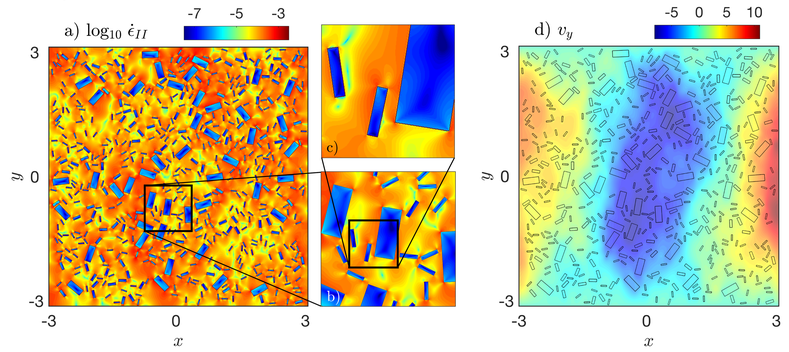

Fig. 4 | High-resolution (5000^2 cells) instantaneous model of crystal-melt settling using a random crystal distribution. (a) The strain rate over the entire model domain (dimensionless). (b) And (c) different figure enlargements and the black frames correspond to the respective areas. (d) The vertical velocity component (dimensionless), each individual crystal is outlined by a black contour line.

> Deformation of heterogenous power law viscous material

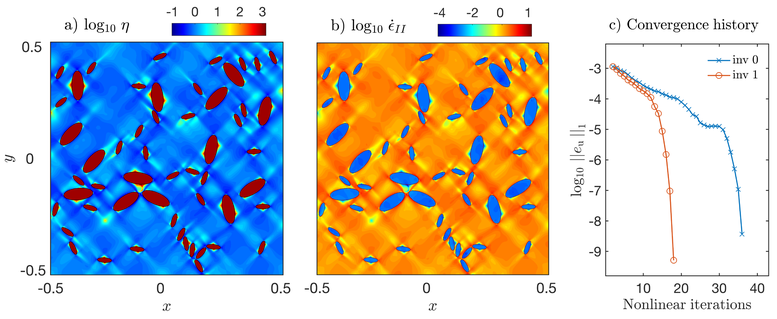

Fig. 5 | Horizontal compression of a material composed of randomly located highly viscous elliptical inclusions in a power law matrix (resolution 1000^2 cells). (a) The resulting effective viscosity and (b) the corresponding strain rate. For the matrix, $\eta_{ref} = 1$ and n=10 and $\eta_{inclusion} = 10^3$. (c) The $\log_{10}$ of the convergence history for the two different definitions of the second strain rate invariant $\dot{\epsilon}_{II}$ as function of nonlinear iteration count. "inv 0" refers to a linear interpolation of the missing strain rate components while "inv 1" refers to a linear interpolation of $\dot{\epsilon}_{II}$ contributions.

> Pressure variation arround a viscous inclusion

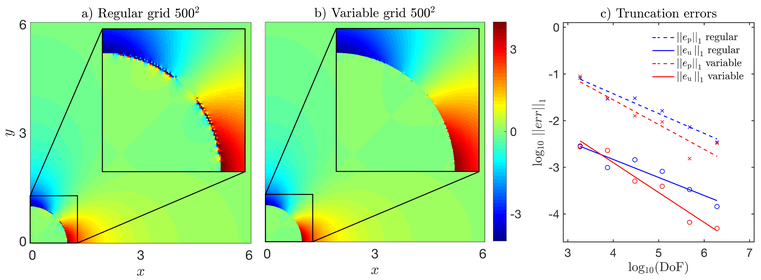

Fig. 6 | (a and b) Computed pressure fields for a single viscous inclusion embedded in constant viscosity matrix using a resolution of 500^2 nodes. The inclusion radius is set to 1, the matrix and inclusion viscosity to 1 and 10^4. (a) Solution obtained with regular grid spacing. (b) Solution computed with variable grid spacing in x and y dimensions. (c) Truncation errors evolution (L1-norm) as function of DoF.

> Mantle flow and dynamic topography in cylindrical coordinates

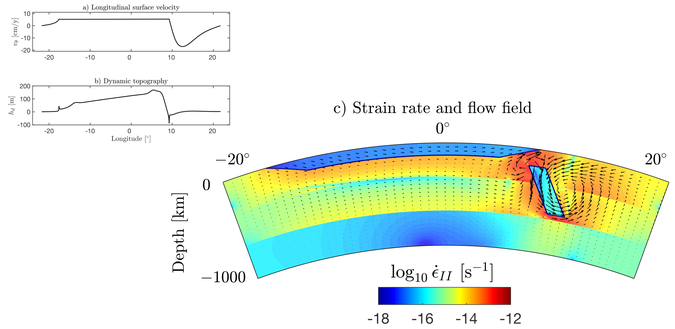

Fig. 7 | Instantaneous model of mantle flow induced by a sinking detached slab in cylindrical coordinates (1000 x 2000 cells). (a) The longitudinal velocity along the surface. (b) The induced dynamic topography. (c) The effective strain rate; arrows correspond to velocity vectors. The dynamic topography (h_{gt}) was calculated according to the relationship $h_t = \frac{-\sigma_{rr}}{g.\Delta\rho}$, where σ_{rr} is the total radial stress (at the surface), g, is the radial component of gravity, and $\Delta\rho$ is the density difference between the lithosphere and the air. The mantle density was set 3250 kg/m^3, its viscosity varies from 10^{19} Pa.s (-330 km), 10^{20} Pa.s (-660 km) and 10^{22} Pa.s (1000 km). The slab and plate densities were, respectively, set to 3275 kg/m^3 and 3245 kg/m^3. Their viscosities were set to 10^{23} Pa.s.

Solver Performance

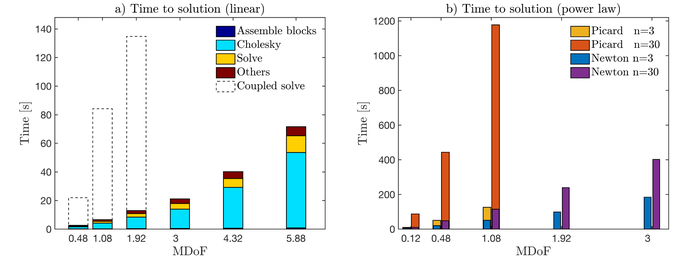

Fig. 8 | Time to solution in seconds for (a) the linear Stokes solver and (b) the power law Stokes solver for both Picard and Newton operators as function of Millions of Degrees of Freedom. In Figure 4a, the wall time of the optimized solve (plain bars) is compared to the wall time of a coupled solve (dashed bars). In Figure 4b, the wall times for nonlinear power law exponents n=3 and n=30 are shown as function of MDoF. The setup used in both Figures 4a and 4b cases is a cylindrical inclusion of high viscosity located in the center of a square domain under simple shear with a background strain equal 1.

Outlook Towards Futur Development

- 22 s for the linear solver and both 180 and 400 s for the nonlinear Newton solver with power law exponent n=3 and n=30, respectively, on a 1000^2 2-D domain.
- Vectorized assembly of matrix operators and solvers relying on efficient sparse Cholesky factorization routines (SuiteSparse).
- The developped mechanical solver can be further extended to address coupled multiphysics problems and design efficient solving procedures or include advection and free-surface.

Adamuszek, M., M. Dabrowski, and D. W. Schmid (2016), Folder: A numerical tool to simulate the development of structures in layered media, J. Struct. Geol., 84, 85–101.

Räss, L., T. Duretz, Y. Y. Podladchikov, and S. M. Schmalholz (2017), M2Di: Concise and efficient MATLAB 2-D Stokes solvers using the Finite Difference Method, Geochem. Geophys. Geosyst., 18, doi:10.1002/ 2016GC006727.